

## Strontium magnesium phosphate, $\text{Sr}_{2+x}\text{Mg}_{3-x}\text{P}_4\text{O}_{15}$ ( $x \sim 0.36$ ), from laboratory X-ray powder data

Jung-Hwa Hong,<sup>a</sup> Seung-Wan Song<sup>b</sup> and Seung-Tae Hong<sup>c\*</sup>

<sup>a</sup>Taejon Christian International School, Daejeon 306-819, Republic of Korea,

<sup>b</sup>Department of Fine Chemical Engineering and Applied Chemistry, Chung-Nam National University, Daejeon 305-764, Republic of Korea, and <sup>c</sup>LG CHEM Research Park, Daejeon 305-380, Republic of Korea

Correspondence e-mail: sthong@lgchem.com

Received 6 October 2010

Accepted 17 November 2010

Online 8 December 2010

The previously unknown crystal structure of strontium magnesium phosphate,  $\text{Sr}_{2+x}\text{Mg}_{3-x}\text{P}_4\text{O}_{15}$  ( $x \sim 0.36$ ), determined and refined from laboratory powder X-ray diffraction data, represents a new structure type. The title compound was synthesized by high-temperature solid-state reaction and it crystallizes in the orthorhombic space group *Cmcm*. It was earlier thought to be stoichiometric  $\text{Sr}_2\text{Mg}_3\text{P}_4\text{O}_{15}$ , but our structural study indicates the nonstoichiometric composition. The asymmetric unit contains one Sr (site symmetry *m* on special position 8g), one *M* (= Mg 64%/Sr 36%; site symmetry *2/m..* on special position 4b), one Mg (site symmetry *2..* on special position 8e), two P (site symmetry *m..* on special position 8f and site symmetry *m* on special position 8g), and six O sites [two on general positions 16h, two on 8g, one on 8f and one on special position 4c (site symmetry *m2m*)]. The nonstoichiometry is due to the mixing of magnesium and strontium ions on the *M* site. The structure consists of three-dimensional networks of  $\text{MgO}_4$  and  $\text{PO}_4$  tetrahedra, and  $\text{MO}_6$  octahedra with the other strontium ions occupying the larger cavities surrounded by ten O atoms. All the polyhedra are connected by corner-sharing except the edge-sharing  $\text{MO}_6$  octahedra forming one-dimensional arrangements along [001].

### Comment

$\text{Sr}_2\text{Mg}_3\text{P}_4\text{O}_{15}:\text{Eu}^{2+}$  was recently reported to show potential for application as a blue phosphor for a white LED under excitation of near-UV light (Ngee *et al.*, 2009; Guo *et al.*, 2010). The existence of a single phase in the system Sr–MgO– $\text{P}_2\text{O}_5$  was first confirmed over 40 years ago (Hoffman, 1968), but only un-indexed X-ray diffraction data were reported and its crystal structure has remained unknown. In the present study, during the course of crystal structure determination, we have discovered that the compound previously known as  $\text{Sr}_2\text{Mg}_3\text{P}_4\text{O}_{15}$  is in fact nonstoichiometric  $\text{Sr}_{2+x}\text{Mg}_{3-x}\text{P}_4\text{O}_{15}$  ( $x \sim 0.36$ ).

We present here its crystal structure, as determined and refined from laboratory powder X-ray diffraction data (Fig. 1).

$\text{Sr}_{2+x}\text{Mg}_{3-x}\text{P}_4\text{O}_{15}$  crystallizes in a new structure type in terms of atomic ratios (6:1:2:15 for tetrahedral–octahedral–ten-coordinated metal–oxygen) and its polyhedral network is, to our knowledge, unique. The structure consists of  $(\text{Mg}_2)\text{O}_4$ ,  $(\text{P}1)\text{O}_4$  and  $(\text{P}2)\text{O}_4$  tetrahedra, and  $\text{MO}_6$  octahedra, where *M* ( $\equiv \text{Mg}1/\text{Sr}2$ ) represents disordered magnesium (Mg1, 64%) and strontium (Sr2, 36%) ions (Fig. 2). The other strontium (Sr1) ions occupy the larger cavities surrounded by O atoms with tenfold coordination (Fig. 3). Each  $(\text{Mg}_2)\text{O}_4$  tetrahedron shares corners with two  $(\text{P}1)\text{O}_4$  and two  $(\text{P}2)\text{O}_4$  tetrahedra.  $(\text{P}1)\text{O}_4$  shares corners with another  $(\text{P}1)\text{O}_4$  (to form a  $\text{P}_2\text{O}_7$  group), two  $(\text{Mg}_2)\text{O}_4$  and one  $\text{MO}_6$  polyhedron.  $(\text{P}2)\text{O}_4$  is connected to only two polyhedra, *viz.*  $(\text{Mg}_2)\text{O}_4$  and  $\text{MO}_6$ . Each O6 atom in the other two corners of the P2 tetrahedron is bonded to two Sr1 ions, one in common to both O atoms. The  $\text{MO}_6$  octahedra form one-dimensional arrangements along [001], sharing edges. Each  $\text{MO}_6$  also shares corners with two opposite-sided  $(\text{P}1)\text{O}_4$  tetrahedra along [010] and four  $(\text{P}2)\text{O}_4$  tetrahedra parallel to the (010) plane. The average *M*–O distance of 2.265 Å is very close to the expected value from the sum of *M* and O ionic radii (2.27 Å) weighted by 64% Mg and 36% Sr (Shannon, 1976).

The empirical expression for bond valence, which has been widely adopted to estimate valences in inorganic solids (Brown, 2002), was used to check the  $\text{Sr}_{2+x}\text{Mg}_{3-x}\text{P}_4\text{O}_{15}$  ( $x \sim 0.36$ ) crystal structure. The bond-valence sums (Brown & Altermatt, 1985; Brese & O’Keeffe, 1991) calculated with the program *VaList* (Wills, 2010) for Sr1 [2.04 v.u. (valence units)],  $(\text{Mg}1/\text{Sr}2)$  (2.30), Mg2 (2.11), P1 (5.06), P2 (4.86), O1 (2.09), O2 (2.12), O3 (2.00), O4 (2.12), O5 (2.20) and O6 (1.85) match the expected charges of the ions reasonably well. The higher valence sum for  $(\text{Mg}1/\text{Sr}2)$  resulted from the shorter Sr2–O

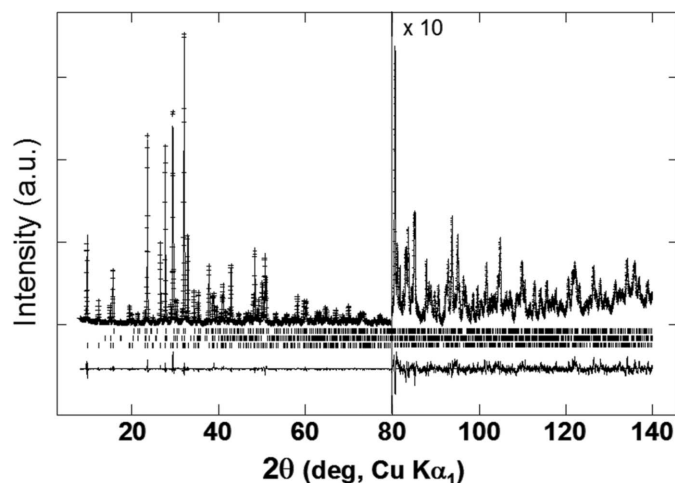


**Figure 1**  
X-ray Rietveld refinement profiles for  $\text{Sr}_{2+x}\text{Mg}_{3-x}\text{P}_4\text{O}_{15}$  ( $x \sim 0.36$ ), including the minor impurity phases, recorded at room temperature. The crossed line marks experimental points and the solid line is the calculated profile. The bottom trace shows the difference curve and the ticks denote expected peak positions for  $\text{Sr}_{2+x}\text{Mg}_{3-x}\text{P}_4\text{O}_{15}$  ( $x \sim 0.36$ ),  $\text{Mg}_2\text{P}_2\text{O}_7$  and  $\text{Mg}_3\text{P}_2\text{O}_8$ , in order from the bottom.

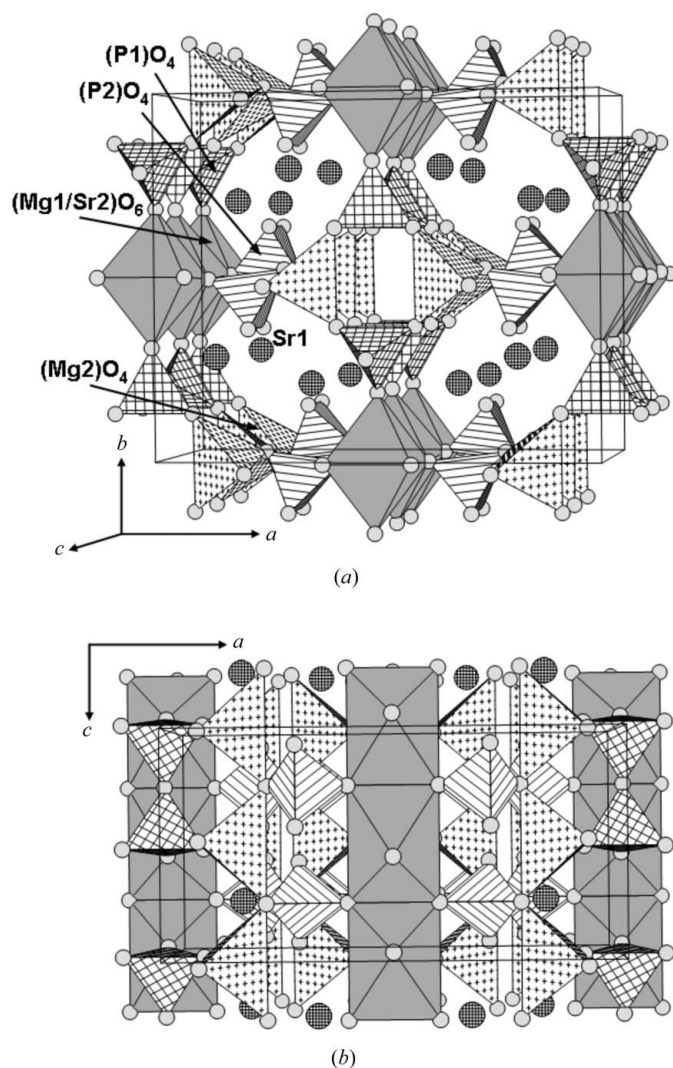


**Figure 2**  
Views of the structure (a) along (001) and (b) along (010), with the unit cell outlined.

bond distances (2.265 Å). All the other interatomic distances are within the expected ranges.

The nonstoichiometry model with more strontium and fewer magnesium ions also conformed to the synthesis results that magnesium phosphates were the impurity phases. Several trials to prepare a single phase  $\text{Sr}_{2+x}\text{Mg}_{3-x}\text{P}_4\text{O}_{15}$  ( $x \sim 0.36$ ) with the nonstoichiometric nominal composition under the same synthesis conditions were unsuccessful: the magnesium phosphate impurities disappeared but instead  $\text{SrMgP}_2\text{O}_7$  (Tahiri *et al.*, 2002) appeared as an impurity phase in the X-ray diffraction pattern. The relative atomic stoichiometries of  $\text{Sr}_{2.36}\text{Mg}_{2.64}\text{P}_4\text{O}_{15}$  and  $\text{SrMgP}_2\text{O}_7$  are quite similar and they seemed to compete with each other kinetically and/or thermodynamically in our synthetic conditions. More careful work should be undertaken to determine reproducible synthetic conditions for the single phase, which is beyond the purpose of the present study.

The crystal structure of  $\text{SrMgP}_2\text{O}_7$  is rather simple compared to  $\text{Sr}_{2.36}\text{Mg}_{2.64}\text{P}_4\text{O}_{15}$ . It consists of  $\text{PO}_4$  tetrahedra,  $\text{MgO}_5$  square-pyramids and eight-coordinated strontium ions

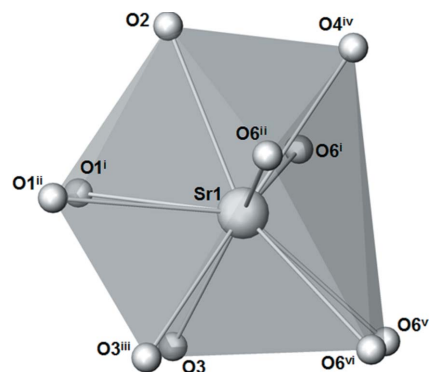


**Figure 3**  
The local environment of strontium (Sr1). [Symmetry codes: (i)  $x, 1 - y, -z$ ; (ii)  $x, 1 - y, \frac{1}{2} + z$ ; (iii)  $x, y, \frac{1}{2} - z$ ; (iv)  $\frac{1}{2} - x, \frac{1}{2} + y, z$ ; (v)  $\frac{1}{2} - x, y - \frac{1}{2}, z$ ; (vi)  $\frac{1}{2} - x, y - \frac{1}{2}, \frac{1}{2} - z$ .]

occupying the larger cavities surrounded by O atoms. Each  $\text{PO}_4$  shares corners with another  $\text{PO}_4$  [to form a  $\text{P}_2\text{O}_7$  group, similar to (P1) $\text{O}_4$  in  $\text{Sr}_{2.36}\text{Mg}_{2.64}\text{P}_4\text{O}_{15}$ ] and three  $\text{MgO}_5$  polyhedra. All five corners of  $\text{MgO}_5$  are connected to  $\text{PO}_4$  tetrahedra. There is no  $\text{MgO}_4$  tetrahedron or octahedron in this structure, unlike  $\text{Sr}_{2.36}\text{Mg}_{2.64}\text{P}_4\text{O}_{15}$ .

## Experimental

$\text{Sr}_{2+x}\text{Mg}_{3-x}\text{P}_4\text{O}_{15}$  ( $x \sim 0.36$ ) was synthesized by a solid-state reaction from a mixture of high-purity  $\text{SrCO}_3$  (99.994%, Alfa Aesar),  $\text{MgO}$  (99.0%, Yakuri Pure Chemicals) and  $(\text{NH}_4)_2\text{HPO}_4$  (99.0%, Junsei Chemical) with a nominal composition of  $\text{Sr}:\text{Mg}:\text{P} = 2.3:4$ . The mixture was thoroughly ground in an agate mortar, dried, pressed into a pellet, heated in air at 1303 K for 4 h, and again at 1323 K for 4 h with intermediate grinding and pressing. The yield was about 90% by weight. The nonstoichiometric composition of the major phase,  $\text{Sr}_{2+x}\text{Mg}_{3-x}\text{P}_4\text{O}_{15}$  ( $x \sim 0.36$ ), was determined later by the structural refinement, and the minor impurity phases were determined to be  $\text{Mg}_2\text{P}_2\text{O}_7$  (Calvo, 1967) and  $\text{Mg}_3\text{P}_2\text{O}_8$  (Nord & Kierkegaard, 1968).

### Crystal data

$\text{Sr}_{2.36}\text{Mg}_{2.64}\text{P}_4\text{O}_{15}$	$V = 1207.83 (1) \text{ \AA}^3$
$M_r = 634.65$	$Z = 4$
Orthorhombic, $Cmcm$	Cu $K\alpha_1$ radiation
$a = 14.27366 (9) \text{ \AA}$	$\lambda = 1.5406 \text{ \AA}$
$b = 11.75678 (7) \text{ \AA}$	$T = 296 \text{ K}$
$c = 7.19753 (4) \text{ \AA}$	flat sheet, $20 \times 20 \text{ mm}$

### Data collection

Bruker D8 Advance diffractometer	Scan method: step
Specimen mounting: packed powder pellet	$2\theta_{\min} = 8.0^\circ$ , $2\theta_{\max} = 140.42^\circ$ , $2\theta_{\text{step}} = 0.02^\circ$
Data collection mode: reflection	

### Refinement

$R_p = 0.048$	$R(F^2) = 0.04372$
$R_{\text{wp}} = 0.063$	$\chi^2 = 6.250$
$R_{\text{exp}} = 0.025$	7939 data points
$R_{\text{Bragg}} = 0.047$	81 parameters
$R(F) = 0.028$	

The powder X-ray diffraction (XRD) data were collected at room temperature on a Bragg–Brentano diffractometer (Bruker AXS Advance D8) with a Cu X-ray tube, a focusing primary Ge(111)

monochromator ( $\lambda = 1.5406 \text{ \AA}$ ) and a position-sensitive Văntec detector with a  $6^\circ$  slit. Data acquisition covered the angular range  $8^\circ \leq 2\theta \leq 140^\circ$  at a step width of  $0.016682^\circ$  and a total measurement time of 40 h. The structure determination from the powder XRD data was performed using a combination of the powder profile refinement program *GSAS* (Larson & Von Dreele, 2000) and the single-crystal structure refinement program *CRYSTALS* (Betteridge *et al.*, 2003). For a three-dimensional view of the Fourier density maps, *MCE* was used (Rohlíček & Hušák, 2007). The XRD pattern was indexed using the program *DICVOL91* (Boultif & Louër, 1991) run in *CRYSTFIRE* (Shirley, 2002) via the positions of 20 diffraction peaks after excluding the impurity peaks, resulting in an orthorhombic unit cell. The systematic absences suggested three possible space groups: *Cmc*<sub>21</sub>, *C2cm* and *Cmcm*. All of them would have resulted in basically the same structure, thus the space group *Cmcm* with the highest symmetry was chosen for the final refinement. LeBail fitting was carried out for the previously unknown phase of  $\text{Sr}_{2-x}\text{Mg}_{3-x}\text{P}_4\text{O}_{15}$ , while Rietveld fitting was carried out for the two known impurity phases.

The structure determination was performed in the same way as in our previous work (Lee & Hong, 2008), where the details are described. At the beginning, a structural model with only a dummy atom at an arbitrary position in the unit cell was used. Structure factors were extracted from the powder data, then direct methods were used for the initial solution of the structure using *SHELXS* (Sheldrick, 2008) run in *CRYSTALS*, which yielded several metal positions. However, not all the atoms could be identified at once. The partial model at this stage replaced the initial dummy-atom model, and was used for a LeBail fit in *GSAS*. Then, improved structure factors were extracted, which were used for the improved data in the refinement in *CRYSTALS*. These processes were iterated until a complete and satisfactory structural model was obtained. Finally, Rietveld refinement was employed to complete the structure determination. Up to this step, a stoichiometric composition of  $\text{Sr}_2\text{Mg}_3\text{P}_4\text{O}_{15}$  was assumed for the unknown phase, and indeed the crystallographic sites ratio seemed to conform to the stoichiometry. However, the displacement parameter of the Mg1 site went to a very small value, and Mg1–O distances (*ca* 2.3 Å) were longer than expected (2.10 Å), but much shorter than the 2.56 Å expected for *d*(Sr–O) from ionic radii (Shannon, 1976). Therefore, it was assumed that some magnesium is substituted by strontium in the Mg1 site, and Sr2 and Mg1 occupancies were refined with a constraint that the displacement parameters for the *M* (Mg1/Sr2) and Mg2 sites were the same, resulting in a dramatic improvement in refinement ( $wR_p$  factors decreased from 16.8 to 6.3%) with reasonable displacement parameters. Lowering the symmetry to *Cmc*<sub>21</sub> or *C2cm* did not separate the problematic Mg1 site, and thus should not make any difference to

this outcome. For the impurity phases, only the cell parameters and scale factors were refined while the other variables were fixed in the final refinement. The overall fit ( $wR_p = 6.3\%$ ) is shown in Fig. 1.

For all compounds, data collection: *COMMANDER* (Bruker, 2003); cell refinement: *GSAS* (Larson & Von Dreele, 2000); data reduction: *EVA* (Bruker, 2003); program(s) used to solve structure: *SHELXS* (Sheldrick, 2008) and *CRYSTALS* (Betteridge *et al.*, 2003); program(s) used to refine structure: *GSAS*; molecular graphics: *ATOMS* (Dowty, 2000); software used to prepare material for publication: *GSAS*.

This work was carried out as a TCIS student research project.

Supplementary data for this paper are available from the IUCr electronic archives (Reference: SQ3270). Services for accessing these data are described at the back of the journal.

## References

- Betteridge, P. W., Carruthers, J. R., Cooper, R. I., Prout, K. & Watkin, D. J. (2003). *J. Appl. Cryst.* **36**, 1487.
- Boultif, A. & Louër, D. (1991). *J. Appl. Cryst.* **24**, 987–993.
- Brese, N. E. & O'Keeffe, M. (1991). *Acta Cryst.* **B47**, 192–197.
- Brown, I. D. (2002). *The Chemical Bond in Inorganic Chemistry*. Oxford University Press.
- Brown, I. D. & Altermatt, D. (1985). *Acta Cryst.* **B41**, 244–247.
- Bruker (2003). *COMMANDER* and *EVA*. Bruker AXS Inc., Karlsruhe, Germany.
- Calvo, C. (1967). *Acta Cryst.* **23**, 289–295.
- Dowty, E. (2000). *ATOMS for Windows*. Version 5.1. Shape Software, 521 Hidden Valley Road, Kingsport, TN 37663, USA.
- Guo, C., Ding, X., Luan, L. & Xu, Y. (2010). *Sens. Actuators B*, **143**, 712–715.
- Hoffman, M. V. (1968). *J. Electrochem. Soc.* **115**, 560–563.
- Larson, A. C. & Von Dreele, R. B. (2000). *General Structure Analysis System (GSAS)*. Los Alamos National Laboratory Report LAUR 86-748, USA.
- Lee, E.-J. & Hong, S.-T. (2008). *J. Solid State Chem.* **181**, 2930–2934.
- Ngee, H. L., Hatsumori, T., Uematsu, K., Ishigaki, T., Toda, K. & Sato, M. (2009). *Phys. Procedia*, **2**, 171–183.
- Nord, A. G. & Kierkegaard, P. (1968). *Acta Chem. Scand.* **22**, 1466–1474. ICSD (Inorganic Crystal Structure Database) No. 31005, version 2009-2, Karlsruhe, Germany.
- Rohlíček, J. & Hušák, M. (2007). *J. Appl. Cryst.* **40**, 600–601.
- Shannon, R. D. (1976). *Acta Cryst.* **A32**, 751–767.
- Sheldrick, G. M. (2008). *Acta Cryst.* **A64**, 112–122.
- Shirley, R. (2002). *The CRYSTFIRE 2002 System for Automatic Powder Indexing: User's Manual*. Guildford, England: The Lattice Press.
- Tahiri, A. A., Bali, B. E., Lachkar, M., Ouarsal, R. & Zavalij, P. Y. (2002). *Acta Cryst.* **E58**, i9–i11.
- Wills, A. S. (2010). *VaList*. Version 4.0.0. Program available from www.CCP14.ac.uk. University College London, London, England.